DIMENSIONING OF A CYLINDRICAL HIGH-PRESSURE MOVABLE GASKET USING THE FINITE ELEMENTS METHOD

Miroslav S. Petrov, Hirsito Slavchev

Technical University, Gabrovo, BULGARIA,

Abstract: Special configurations of gaskets are used in hydro systems working at extremely high pressures. The present article deals with such a movable cylindrical gasket that comprises a body – thick-walled tube and a cover –thin-walled tube in the gasket area. Relations are derived concerning the inner stress state of the thick-walled tube depending on the outer diameter of the tube facilitating the choice of the latter. The alterations of the values of the stresses in the contact surface, the body and the cover are examined using the Finite Elements Method (FEM). Some constructive suggestions are presented in the article that will lower the values of the contact stresses in the cylindrical gasket.

Keywords: *high-pressure movable gasket*, **F**inite **E**lements **M**ethod (FEM), hydro systems working

1. INTRODUCTION

The technological operations in high-pressure processes demand special requirements for the gaskets in terms of relatively more sophisticated constructions for pressures in the interval from 500 up to 1000 MPa. This is the case for the congestion of a movable cover of isostatic chambers. Technologically the isostatic action of extremely high pressures is used for pressing of not readily flammable metallic powders. The metallic powder is placed in a cylindrical container which is situated in the pressing chamber through a movable cover. When the cover is in position the pressure in the chamber is being increased up to 500 - 1000 MPa, then follows a detention and a decrease of the pressure. Then the elastic container is being ejected from the pressing chamber.

The congestion of the cover with the isostatic chamber is realized by a special construction of a cylindrical gasket. The corpus of the isostatic chamber is presented by a thick-walled tube which inner diameter works as a congesting surface.

The movable cover has a special construction. The upper part is formed as a solid cylinder and the lower part is a thin-walled tube with outer diameter of D_2 =100 mm which realizes the congestion and inner diameter of D_1 =90 mm and height of the elastic part of H= 100 mm. On the outer surface of the cover congestion there are three grooves with depth of 0,5 mm and height of h=0,5 mm. The windage between the body and the cover in the congestion zone is δ =0,01 mm. At increase of the pressure in the isostatic chamber the thin-walled cylinder deforms and congests at its outer diameter the inner diameter of the thick-walled cylinder.

2. AIM OF THE RESEARCH WORK

The aim of the article is by using the FE Method to analyze the distribution of the:

- radial σ_r , tangential σ_t , axial σ_z μ equivalent $\sigma_{e\kappa e}^{IV}$ stresses in the body of the thick-walled cylinder at fixed inner radius of R_1 =50 mm and variation of the outer radius R_2 from 80 to 300 mm.
- radial contact stresses σ_r , at different height of the groove h=5, 4, 3 μ 1,5 mm.

3. CLASICS RESULTS

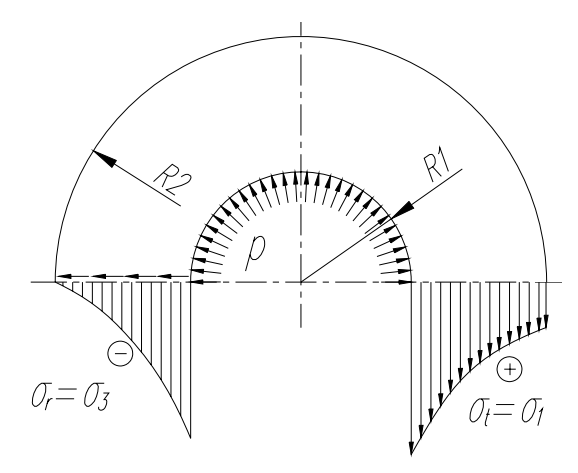


Fig.1 Diagram of the distribution of the principle stresses in the walls of the thick-walled tube

The classical method for dimensioning of a thick-walled tube is used to solve these problems. Fig. 1 shows the meridian section of the chamber where the radii and the principal stresses $\sigma_r = \sigma_3$, $\sigma_t = \sigma_1$ are marked at the state of uniform loading with inner pressure p.

The most endangered points are those on the inner surface where the principle stresses are:

$$\sigma_1 = \sigma_t$$
; $\sigma_2 = \sigma_z$; $\sigma_3 = \sigma_r$ (1)

The classical relations defining the stresses at a random point of the tube section are presented as a function of the radii on the analyzed point r.

$$\frac{\sigma_r(r)}{\sigma_t(r)} = \frac{pR_1^2}{R_2^2 - R_1^2} \left(1 \mp \frac{R_2^2}{r} \right)$$
 (2)

$$\sigma_z(r) = \frac{pR_1^2}{R_2^2 - R_1^2} \tag{3}$$

The extreme values are:

$$\begin{split} &\sigma_{r,R_1} = -p_{R_1}; & \sigma_{r,R_2} = 0; \\ &\sigma_{t,R_1} = p_{R_1} \frac{R_2^2 + R_1^2}{R_2^2 - R_1^2}; & \sigma_{t,R_2} = p_{R_1} \frac{2R_1^2}{R_2^2 - R_1^2} = 2\sigma_z. \end{split} \tag{4}$$

For the equivalent stresses according the IV-th theory for strength we have:

$$\sigma_{e_{KG.}}^{IV} = \sqrt{\sigma_1^2 + \sigma_2^2 + \sigma_3^2 - \sigma_1 \sigma_2 - \sigma_2 \sigma_3 - \sigma_3 \sigma_1} = p_{R_1} \frac{\sqrt{3}R_1^2}{R_2^2 - R_2^2} \le \sigma_{\partial on.}$$
 (5)

For dimensioning of the outer diameter R₂ at fixed inner one R₁ and maximal pressure p one can use:

$$\therefore \frac{R_1}{R_2} \le \sqrt{\frac{\sigma_{oon.} - 2p_{R_1}}{\sigma_{oon.}}} \Rightarrow R_2^{IV} \le \sqrt{\frac{\sigma_{oon.}}{\sigma_{oon.} - \sqrt{3}p_{R_1}}}.$$
 (6)

Fig.2 shows the distribution of the normal radial stresses $\sigma_r = \Box \sigma_3 [MPa]$ according to the FEM in the wall of the tube at $R_1 = 50$ mm, $R_2 = 80$ mm, loading of p = 1000 Mpa and error with the value of Err=0,17%.

Table I shows the alteration of the normal stresses – tangential $_{max}\sigma_1$ = σ_t , axial σ_2 = σ_z and the equivalent stresses $\sigma^{VonMisses}_{e\kappa e}$ (at normal radial stress $_{max}\sigma_r$ = σ_3 =-p = -1000 MPa) and change of the outer radius R_2 =80 ... 300 mm.

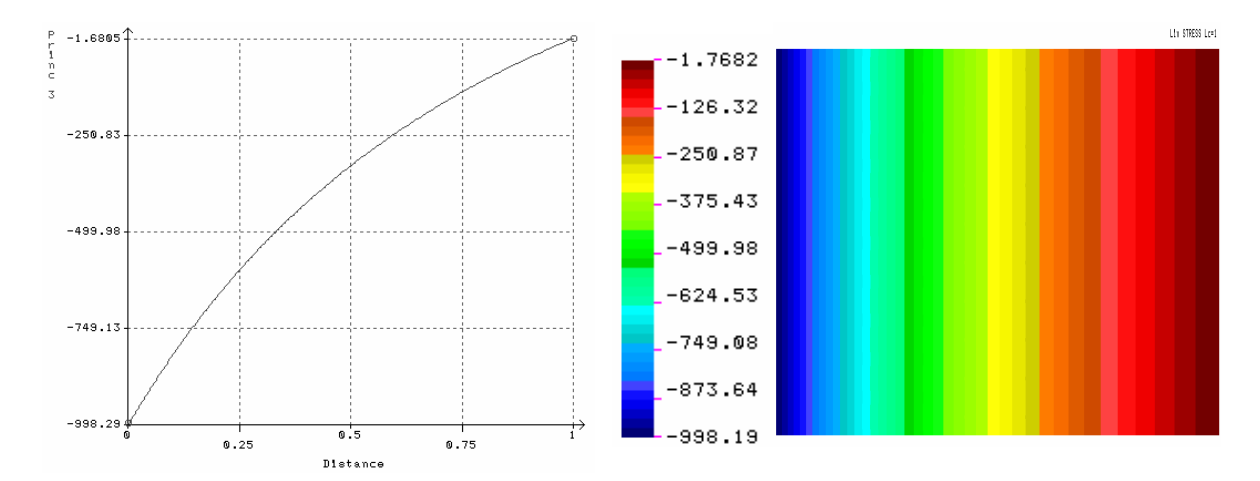


Fig. 2.

Table 1.

R _{out.}	$_{\max}\sigma_1 = \sigma_t$	$\sigma_2 = \sigma_z$	max o Von Misses	R _{out.}	$_{\max}\sigma_1=\sigma_t$	$\sigma_2 = \sigma_z$	$_{max}\sigma^{VonMisses}$
[mm]	[MPa]	[MPa]	[MPa]	[mm]	[MPa]	[MPa]	[MPa]
80	2282,05	641,03	2842,34	195	1140,75	70,37	1853,94
85	2058,20	529,10	2648,48	200	1133,33	66,67	1847,52
90	1892,86	446,43	2505,29	205	1126,50	63,25	1841,60
95	1766,28	383,14	2395,67	210	1120,19	60,10	1836,14
100	1666,67	333,33	2309,40	215	1114,35	57,18	1831,08
105	1586,51	293,26	2239,98	220	1108,93	54,47	1826,39
110	1520,83	260,42	2183,11	225	1103,90	51,95	1822,03
115	1466,20	233,10	2135,79	230	1099,21	49,60	1817,97
120	1420,17	210,08	2095,93	235	1094,83	47,42	1814,18
125	1380,95	190,48	2061,97	240	1090,74	45,37	1810,64
130	1347,22	173,61	2032,75	245	1086,92	43,46	1807,32
135	1317,97	158,98	2007,42	250	1083,33	41,67	1804,22
140	1292,40	146,20	1985,27	255	1079,97	39,98	1801,31
145	1269,91	134,95	1965,80	260	1076,80	38,40	1798,57
150	1250,00	125,00	1948,56	265	1073,83	36,91	1795,99
155	1232,29	116,14	1933,22	270	1071,02	35,51	1793,56
160	1216,45	108,23	1919,50	275	1068,38	34,19	1791,27
165	1202,22	101,11	1907,18	280	1065,88	32,94	1789,10
170	1189,39	94,70	1896,07	285	1063,51	31,76	1787,05
175	1177,78	88,89	1886,01	290	1061,27	30,64	1785,12
180	1167,22	83,61	1876,87	295	1059,15	29,58	1783,28
185	1157,60	78,80	1868,54	300	1057,14	28,57	1781,54
190	1148,81	74,40	1860,92				

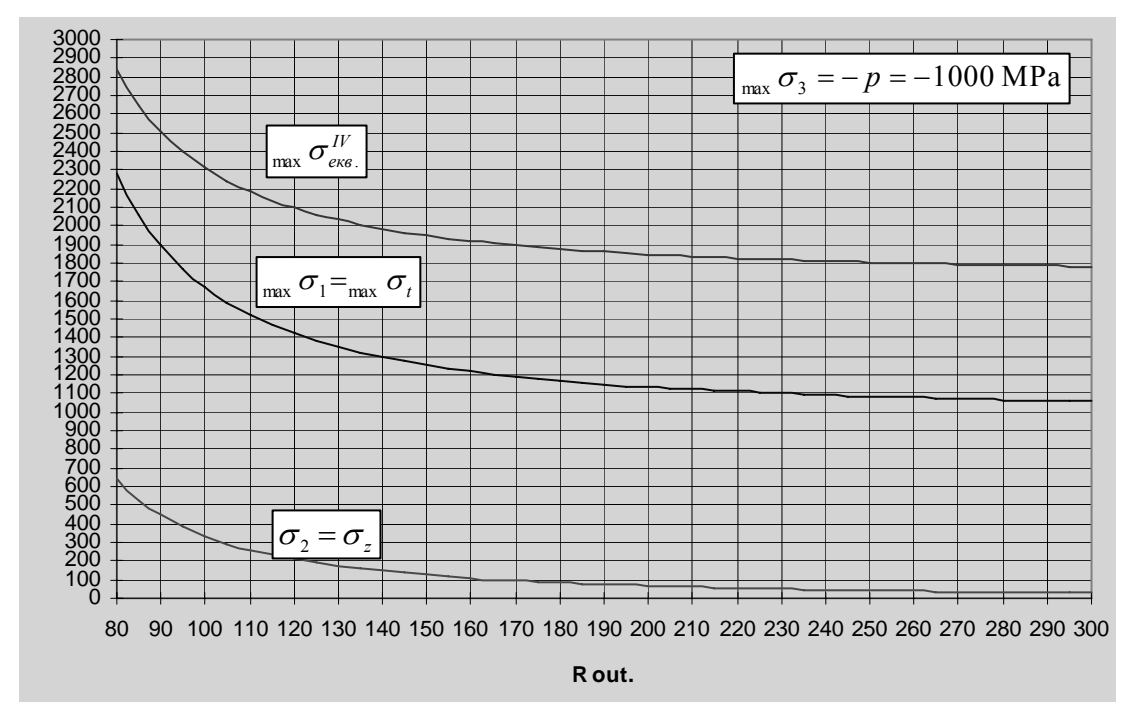


Fig. 3.

Fig. 3 shows a diagram that can be used for choosing of the outer radius of a thick-walled tube (R_{out}) or material according $_{max}\sigma_{eq} \le \sigma_{adm}$ for pressure with the value of p=1000MPa and inner radius $R_{inn.}$ =50 mm. Analyzing the alteration of R_2 one can say that for values R_2 =80 ... 200 mm there is a steep profile of the alteration diagram and a choice in this interval will present an effective solution; for values R_2 =200 ... 300 mm the alteration of σ is light and this area can be assessed as non-effective. This graphical inquiry allows at a choice of the material for the body to specify the magnitude of R_2 and vice versa.

4. RESULTS FROM THE FEM CALCULATION

A constructive parametrical scheme is made aiming to estimate the stress distribution in the meridian section of the body of the chamber and of the cover, which is shown on Fig. 4.

The parameters in fig. 4 have the following physical meaning: - Inner radius of the cylinder Rw = 50 mm;

- Thickness of the elastic wall of the cover WWT = 5 mm; Height of the elastic cylindrical part pf the cover Hg = 100 mm; Height of the groove Hm = 5 mm; Number of grooves Nk = 3;
- Depth of the groove and fillet radius Zl = 0.5 mm; Fillet radius Dg = 7 mm; Outer radius of the cover Rk = 120 mm; Height of the cover Hk = 20 mm; Outer radius of the conical opening Rs = 5 mm; Radius of the tube for the fluid flow Ro = 2 mm; Difference of the heights of the inner bottom of the Hob = 5 mm; Inner fillet radius of the cover bottom Rz = 10 mm; Average size of the finite element of the cover Esiz1 = 1 mm; Average size of the finite element of the cylinder Rwan = 160 mm; Examined slice of the height of the cylinder Rwan = 1.2*Hg; Windage of contact Rwan = 1.2*Hg; Windage

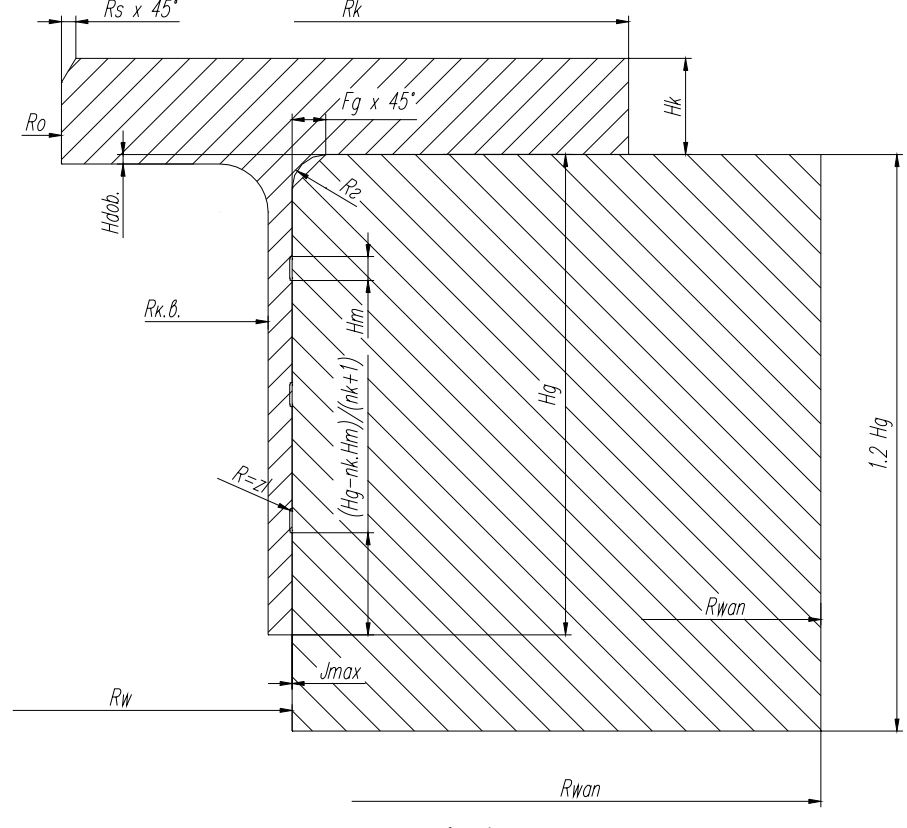


Fig. 4.

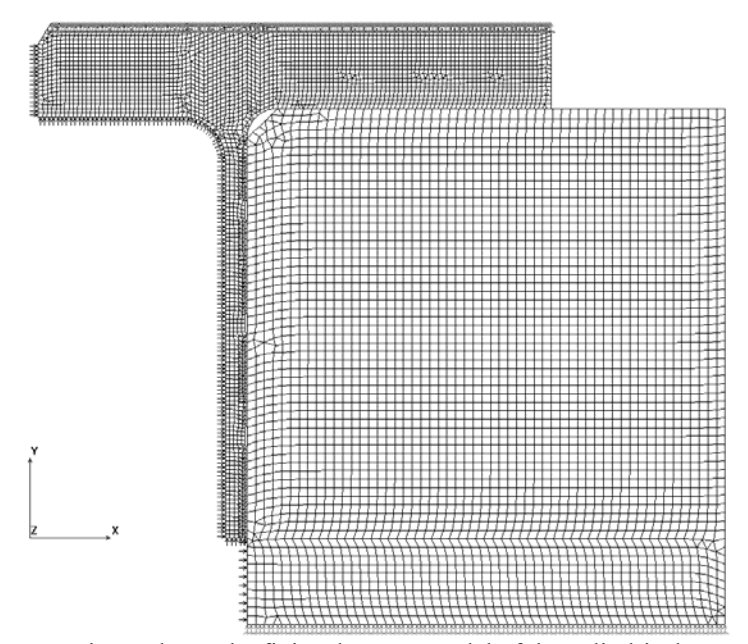


Fig. 5. shows the finite elements model of the cylindrical

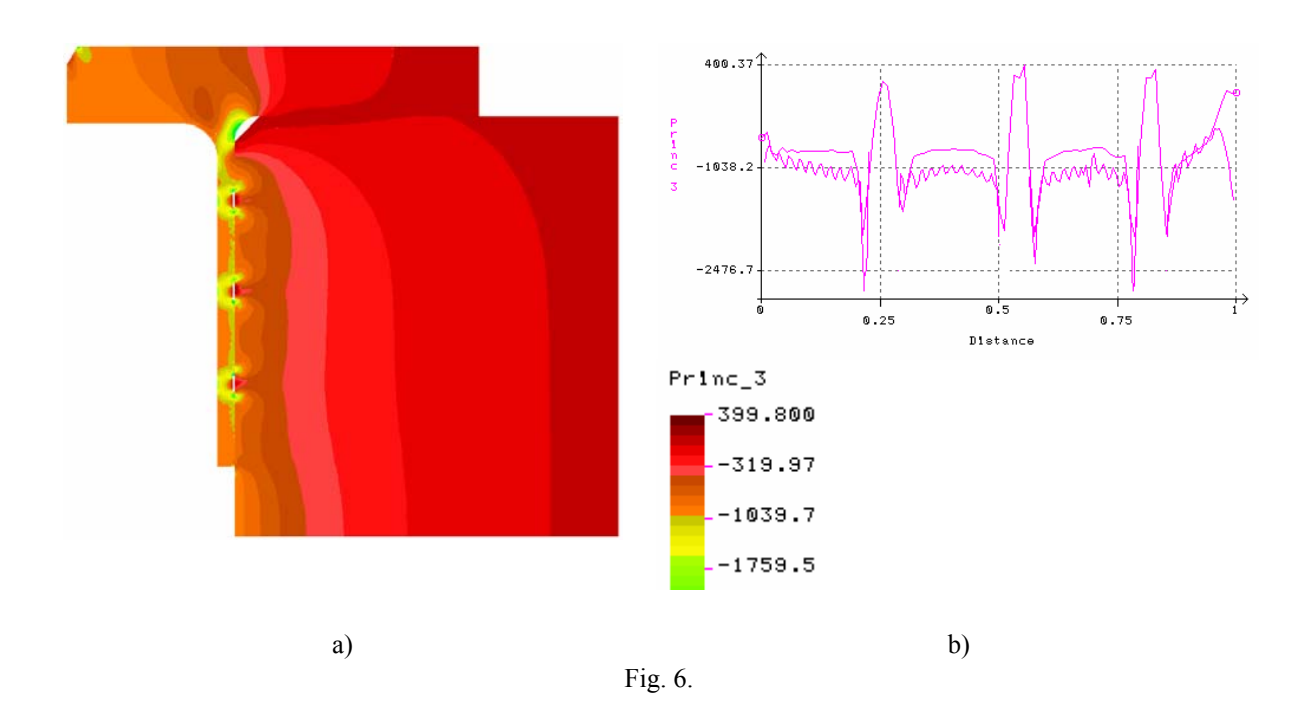
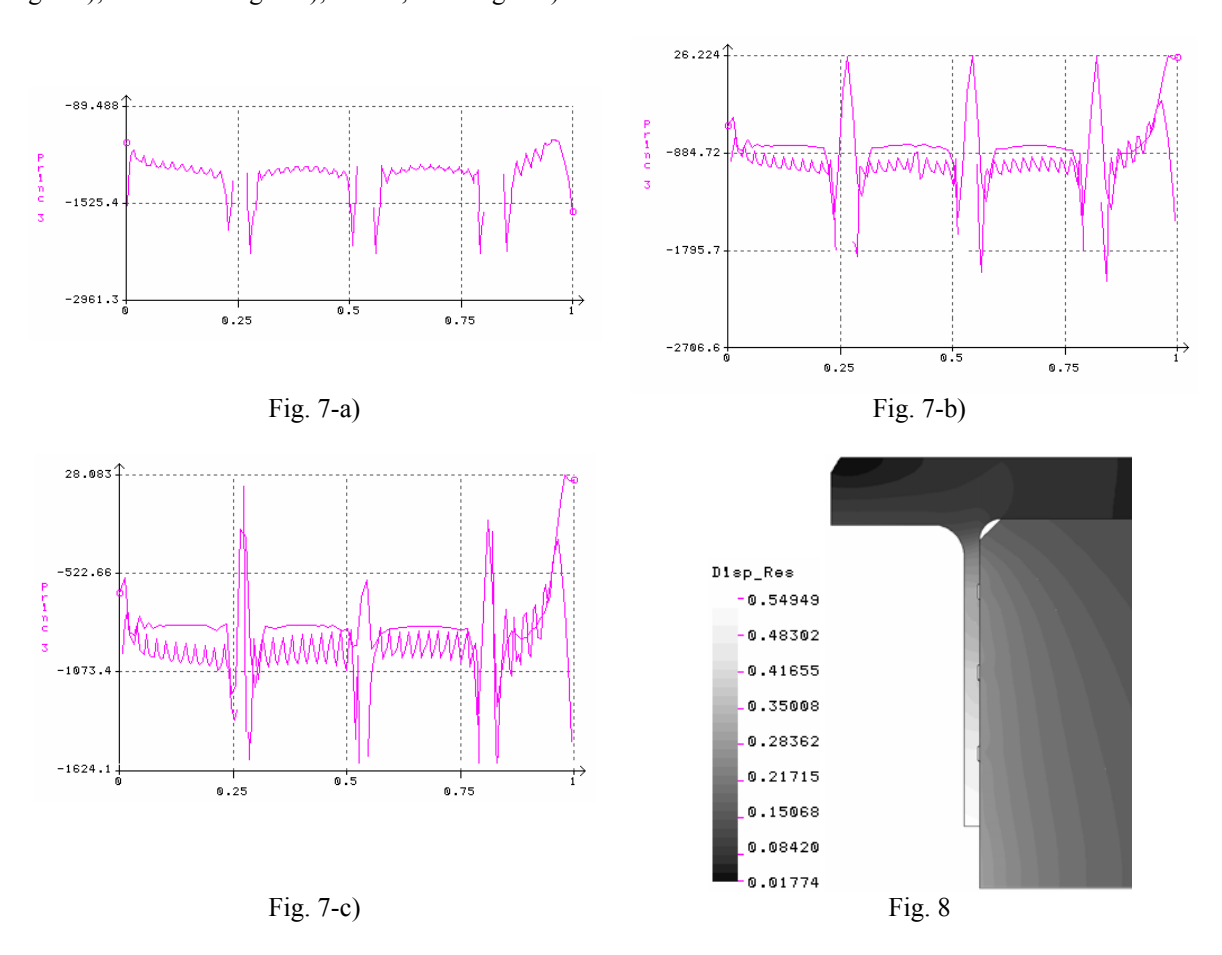


Fig. 7 shows graphically the distribution of $\sigma_r = \sigma_3$ along the contact surface at: height of the groove Hm=4 mm fig. 7 a); Hm=3 mm fig. 7 b); Hm=1,5 mm fig. 7 c).



The pressure is given for all inner edges and the fastening is chosen to be close to the scene of contact because the stresses in vertical direction $\sigma_z = \sigma_2$ are evenly distributed in the section. Two regions are used for the analysis filled with axis-symmetrical finite elements PLANE2D.

Automatically generated GAP finite elements and contact lines are applied on the surface of the contacting elements of the axis-symmetrical model, which realize the solution of the problem of contact.

The FEM analysis is carried out by COSMOS as a non-linear contact problem. Fig. 6 shows the distribution of $\sigma_r = \sigma_3$ in the meridian half-section of the contacting elements at height of the groove Hm=5 mm – Fig. 6 a), and graphically the alteration of $\sigma_r = \sigma_3$ on the contact surface on fig. 6 b).

Fig. 6 b) explicitly shows the extreme values situated closely to the outer side of the three grooves, which assure the hermeticity of the connection i.e. they have values greater than the working p=1000 MPa.

Fig. 8 shows the distribution of the deformations in the right meridian half-section of the contacting elements in millimeters at Hm=5 mm.

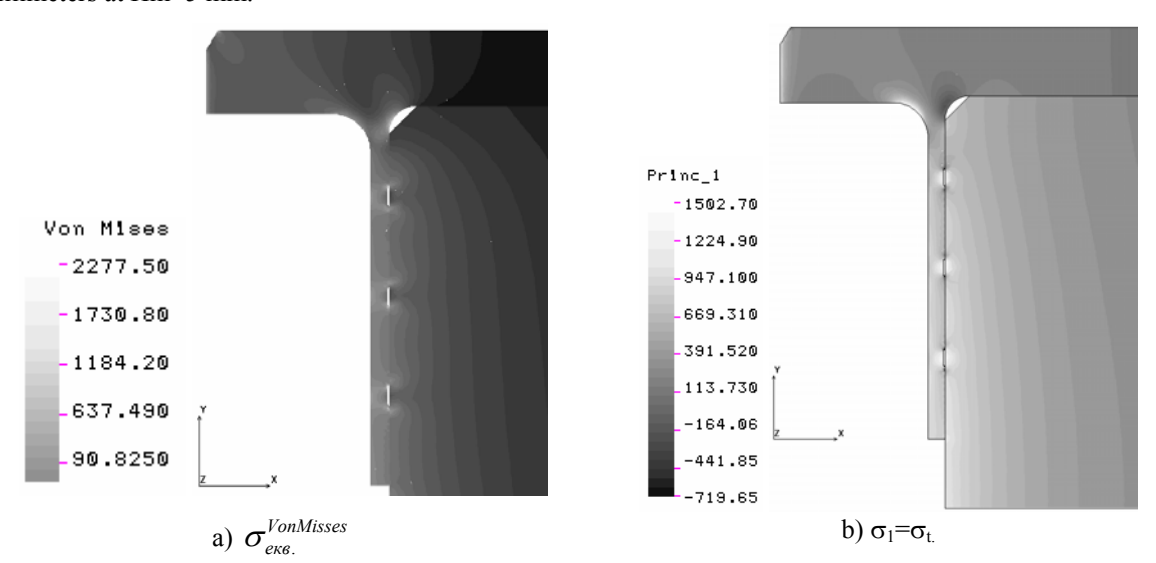


Fig. 9. Distribution of the stresses in the right meridian half-section of the contacting elements at Hm=5 mm

5. CONCLUSIONS

From the research that was carried out and from the illustrations on the figures the following conclusions can be made:

- the contact stresses that are obtained have their extreme values which exceed the loading stress from the pressure p=1000MPa, which guarantees the hermeticity of the connection;
- the stress concentration is observed in the transient sections. To lower their magnitude to the admissible ones it is necessary to use suitable fillet radii, which is made in the parametric scheme on fig. 4. Such radii are: $R_Z=10$ mm and ZI=0.5 mm;
- the values of the stresses σ_r , σ_t in $\sigma_{e\kappa\theta}^{VonMisses}$ of the contacting elements are given, which values can be read from the different colours of the printout;
- the alterations of the normal stresses of the contacting elements is given at different height of the groove Hm=5; 4; 3; 1.5 mm, and the results are presented graphically.

6. CONTRIBUTIONS

As a conclusion it can be stated that the required problems are solved, i.e.:

- according to the graphical relations on fig. 3 a material is chosen with specific admissible stresses and subsequently the outer diameter of the thick-walled tube D_2 is obtained and vice versa;
- using the FE method the stresses σ_r , σ_t , $\sigma_{e\kappa\theta}^{VonMisses}$ are obtained in the elements of the congestion;
- the initial construction is corrected by filleting of the transitional elements and the stresses are lowered to the admissible values for contact stresses of the material. In the line of contact the stresses exceed the working pressure p = 1000 MPa.

REFERENCES

- [1] Cosmos/M Finite Element Analysis User Guide (Vol. 1), SRAC, 1994.
- [2] Cosmos/M The Basic System, SRAC, 1994.
- [3] Cosmos/M Command Reference, SRAC, 1994.
- [4] Cosmos/M Advanced Modules, SRAC, 1994.
- [5] Kiseov I. Handbook of engineer, part II Mechanics, Sofia, Technika, 1978. (in Bulgarian)
- [6] Kiseov I. Strength of materials. Sofia, Technika, 1978. (in Bulgarian)